High-energy quasielastic $\nu_\mu n \to \mu^- p$ scattering in deuterium

T. Kitagaki, S. Tanaka, H. Yuta, K. Abe, K. Hasegawa,
A. Yamaguchi, K. Tamai, T. Hayashino, Y. Otani, H. Hayano, and H. Sagawa
Tohoku University, Sendai 980, Japan

R. A. Burnstein, J. Hanlon, and H. A. Rubin
Illinois Institute of Technology, Chicago, Illinois 60616

C. Y. Chang, S. Kunori, G. A. Snow, D. Son,* P. H. Steinberg, and D. Zieminska†
University of Maryland, College Park, Maryland 20742

R. Engelmann, T. Kafka, and S. Sommars‡
State University of New York at Stony Brook, Stony Brook, New York 11974

C. C. Chang,§ W. A. Mann, A. Napier, and J. Schneps
Tufts University, Medford, Massachusetts 02155
(Received 13 December 1982)

We have studied the quasielastic reaction $\nu_\mu n \to \mu^- p$ in an exposure of the Fermilab deuterium-filled 15-foot bubble chamber to a high-energy wide-band neutrino beam. From an analysis of the Q^2 distribution based on the standard $V-A$ theory, the axial-vector mass in a dipole parametrization of the axial-vector form factor is determined to be $M_A = 1.05^{+0.12}_{-0.16}$ GeV, consistent with the values previously reported from low-energy experiments.

I. INTRODUCTION

The weak structure of the nucleon has been studied using the quasielastic neutrino reaction

$$\nu_\mu n \to \mu^- p \tag{1}$$

on both complex nuclei[1] and deuterium[2–4] at neutrino energies less than 10 GeV. In all of these studies the formulation of the standard $V-A$ theory was assumed with a dipole form of the weak axial-vector form factor. Time-reversal invariance, charge symmetry, and the conserved-vector-current (CVC) hypothesis are also assumed to simplify the formulation. Reported values of the axial-vector mass M_A range between 0.65 and 1.07 GeV; the weighted average is somewhat smaller than, but consistent with, the mass value $M_A \sim 1.15$ GeV obtained from electroproduction experiments.[5] These results, as well as the absolute cross section for the quasielastic reaction, are consistently described by the formulation of the $V-A$ theory in the low-energy region. However, there has been no experimental study of the quasielastic reaction at Fermilab energies.

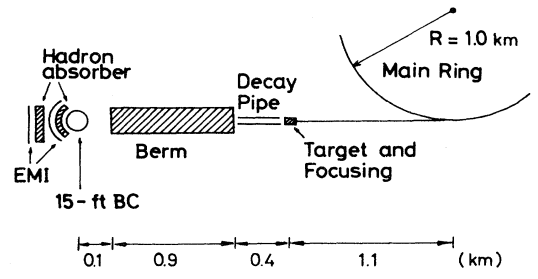

FIG. 1. Schematic layout of the neutrino beam line and the bubble chamber with two-plane external muon identifiers (EMI).

In this paper we present the results of an analysis of the quasielastic events (1) observed in an exposure of the Fermilab 15-ft deuterium-filled bubble chamber to a high-energy wide-band neutrino beam. The main purpose of the present study is to measure the weak axial-vector form factor $F_A(Q^2)$ using the dipole parametrization and to examine the hypothesis that the form factor is energy independent. This extends the study of the $V-A$ formulation to neutrino energies of 100—200 GeV. Earlier results from this experiment have been published elsewhere.[6–10]

II. EXPERIMENTAL DETAILS

A. Neutrino beam and bubble chamber

The wide-band neutrino beam was produced by 350-GeV/c protons striking a 33-cm-long beryllium oxide target. Figure 1 shows the schematic layout of the neutrino beam line. Secondary particles with positive charge were focused by a horn magnet pulsed to a maximum current of 80 kA. The neutrinos were produced from π^+ and K^+ decays in flight in a 400-m-long decay pipe. With the exception of neutrinos, almost all particles which pass through this decay pipe are absorbed in the 900-m-long earth berm and iron shield. Thus at the end of the berm, a beam consisting primarily of ν_μ emerged. The contamination of the neutrino flux by antineutrinos is estimated by a Monte Carlo simulation[11] to be about 14%. The neutrino flux has a maximum at 20 GeV and extends above 200 GeV with an average energy of 27 GeV. A total of 328 000 pictures was taken with 4.9×10^{18} extracted protons, averaging about 1.5×10^{13} protons per pulse. A detailed study of this flux is given in Ref. 10.

The bubble chamber is located at 95 m from the end of the berm. The bubble chamber filled with liquid deuterium at 29 °K was operated with a pressure of 80 psi during the run. The chamber was equipped with six cameras of which three cameras, 4, 5, and 6, were designated for this neutrino run. A superconducting magnet was used, producing a field strength of 3.0 T at the center of the chamber. The two-plane external muon identifier (EMI) was operated downstream of the bubble chamber. The mean absorber thickness in terms of the pion mean free paths is 4 to the first plane and 9 to the second plane.

B. Scanning and measuring procedures

The quasielastic events were collected from a scan for neutral induced events with more than one prong in a fiducial volume defined as

$$(x^2+y^2+z^2)^{1/2} < 175 \text{ cm} ,$$

$$-130 < z < 120 \text{ cm} ,$$

and with additional cuts

$$x > -150 \text{ cm} , \text{ and } x_w - x > 60 \text{ cm for } x > 0 .$$

Here, the x axis of the chamber coordinate system is nearly parallel to the beam direction ($\sim 2.5°$ off-axis), the z axis is directed downward and the origin is at the chamber center. The point (x_w,y,z) lies on the spherical chamber wall at a radius of 188 cm. This yields a total volume of 16.7 m^3 and a target mass of 2 tons. We scanned all usable pictures from 96% of the total exposure, corresponding to 4.76×10^{18} protons on target.

Quasielastic events in deuterium,

$$\nu_\mu d \to \mu^- p p_s , \tag{2}$$

appear as one-prong, two-prong, or three-prong events depending on the momenta of the recoil proton p and spectator proton, p_s. All usable pictures were scanned twice and 80% of them were scanned three times for two- and three-prong events. A correction was made for quasielastic one-prong events as will be discussed later. To reduce low-energy neutral-hadron-induced backgrounds, only events with at least one secondary track with momentum above 1.8 GeV/c were selected by using momentum templates on the scanning tables.

The events were measured and processed through the TVGP-SQUAW program chain. Events that failed our geometrical-reconstruction criteria were remeasured. We accept only those events in the fiducial volume of 16.7 m^3 which have $\Delta p/p < 0.5$ for all tracks and which satisfy the charge balance requirement. We further select only those events with the sum of visible secondary particle momenta greater than 5 GeV/c in the neutrino direction. Two-prong events consistent with an interpretation as γ, K^0, Λ, or $\bar{\Lambda}$ are removed from the event sample. The overall scanning-measuring efficiencies for two- and three-prong events were found to be (89±2)% and (87±2)%, respectively.

C. Selection of the quasielastic sample

Using the kinematic-fitting program SQUAW, the two- and three-prong events are fitted to reaction hypothesis (2). Since the neutrino-beam direction is known to better than 1 mrad, a three-constraint kinematic fit (3C fit) to reaction (2) was made for the two- and three-prong events. If the spectator proton were not visible or unmeasurably short, the 3C fit was performed using a spectator-proton momentum of 0±45 MeV/c as a starting value for the Cartesian components of $\vec{p}_s$. The χ^2 probability distribution is uniform, but shows a spike for the χ^2 probability less than 1% where 16% of the events was found to have an associated gamma or vee. Requiring that the χ^2 probability is greater than 1% and that the particle identification is consistent with reaction (2), we obtained 362 events. Figure 2 shows the spectator momentum distribution for these events. If two protons were observed in the event, the lower-momentum proton was taken to be a spectator. The shaded area represents the observed spectators. The solid curve is the prediction obtained from the Hulthen momentum distribution[12] of the nucleons in the deuteron and the area is normalized to the total number of quasielastic events. A small excess of events with high spectator momentum is seen which may be due to the rescattering of the proton in the deuteron. Rescattered events are included in the sample since they do not affect Q^2. Initial quasielastic events suffering from rescattering may also appear in nonquasielastic topologies such as four- or six-prong events. However, the fraction of such events is estimated to be at most 2%, because most of the rescattering occurs in the momentum region less than 1 GeV/c. No correction was made for this loss.

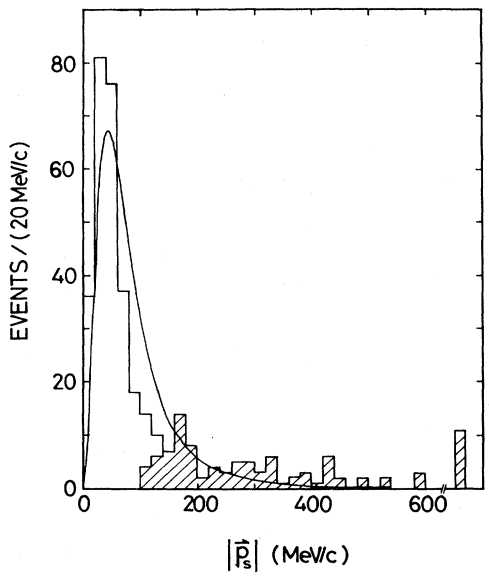

FIG. 2. Spectator-proton momentum distribution for events fit to the reaction $\nu_\mu d \to \mu^- p p_s$. The shaded area displays events with measured spectator momenta and the unshaded area shows events in which the spectator momenta are obtained from the fits. The smooth curve is the prediction of the Hulthen wave function normalized to the total number of quasielastic events.

The Hulthen distribution in Fig. 2 deviates from the data for $|\vec{p}_s| < 160$ MeV/c. This deviation primarily comes from the deficiency in the fit procedure used for the invisible spectator protons. We have examined the

background effect due to different values of the momentum spread. If the spread of ± 60 MeV/c is used, agreement between data and the Hulthen spectator-momentum distribution was improved. However, this increases the background in the sample. Therefore, we used for the invisible spectator protons a spread of ± 45 MeV/c. We note that the discrepancy in the spectator-momentum distribution does not alter the results discussed here except for influencing the background rate in the sample.

In order to check for bias in the two-prong sample, we have investigated the quantity ϵ. The quantity ϵ is defined as

$$\epsilon = E_\mu + E_p - (P_{\mu l} + P_{pl}) - M_n \ , \tag{3}$$

where the subscripts μ, p, and n denote the outgoing muon and proton, and the target neutron, respectively; subscript l denotes the longitudinal momentum component relative to the incident ν_μ direction. The value of ϵ should be negative or zero for the correct mass assignment of each track, ignoring internal motion of the nucleon in the deuteron and measurement error. Figure 3 shows the ϵ distribution for all two-prong events. The shaded area shows the quasielastic events. No significant event loss nor background was observed in the two-prong quasielastic sample. The dashed line, the background for the quasielastic events, was given by normalizing to the unshaded events in the ϵ region between -0.1 and 0.1 GeV, where the line was fixed to be zero at $\epsilon = 0.1$ GeV. The curve was obtained from a Monte Carlo simulation for the quasielastic events and normalized to the shaded events in the same region. The quasielastic events were generated so as to accord with the observed E_ν and Q^2 distributions. The internal motion of the nucleon in the deuteron[12] and the measurement errors were also included in the simulation. As seen in Fig. 3, the quasielastic events are symmetrically distributed about $\epsilon = 0$ as predicted from the Monte Carlo simulation. The broadening of the quasielastic peak primarily comes from the unobserved spectator proton.

D. Background and bias corrections

The possible background in our quasielastic sample comes from both neutral-hadron interactions and inelastic neutrino interactions with undetected neutral particles. The backgrounds induced by neutrons and K^0's were estimated by using the reactions $np \to pp\pi^-$ and $K^0 n \to K^0 p \pi^-$ obtained as 1C fits in the same experiment. Fitting these 1C events to reaction (2), we found no events selected as quasielastic and thus estimated the contamination from these reactions to be less than 1% for $E_\nu > 5$ GeV.

We have also searched for γ's and V^0's associated with events in our quasielastic sample. Three events were found with a single γ, which likely comes from a π^0 in the reaction $\nu_\mu n \to \mu^- p \pi^0$, and one event had a possible associated Λ. These four events were not included in our sample of 362 events. The contamination from similar events when the γ or V^0 is undetected is estimated to be $(4 \pm 3)\%$, using a single-γ detection efficiency of 0.10.[13] Using the observed 3C-fit $\nu_\mu d \to \mu^- p \pi^+ n_s$ events, and replacing the π^+ by π^0, we have estimated the background from the reaction $\nu_\mu d \to \mu^- p \pi^0 p_s$ to be 2%, which is consistent with the above estimate. Similarly, the background from reactions $\nu_\mu d \to \mu^- n \pi^+ p_s$ and $\nu_\mu d \to \nu p \pi^- p_s$ is estimated to be less than 0.5%. We have also examined the contamination from $\bar{\nu}$-induced events in the sample by use of the EMI information and found no μ^+ in the sample.

Figure 4 shows the distribution of the azimuthal angle ϕ of the recoil proton around the incident neutrino direction for the quasielastic events with $Q^2 > 0.1$ GeV^2. The angle ϕ is measured from the plane containing the camera and the ν direction (0° toward the bottom of the chamber) and three points per event (one for each camera) were plotted. An event loss is clearly observed near $\phi = \pm 180°$, but not

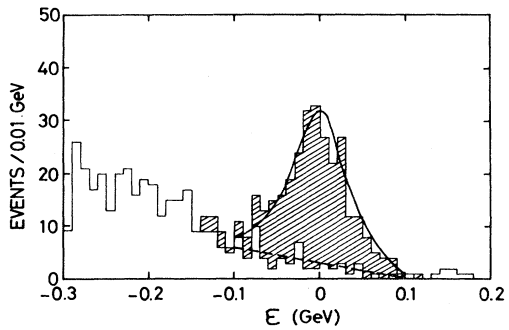

FIG. 3. Distribution of $\epsilon = E_\mu + E_p - (P_{\mu l} + P_{pl}) - M_n$ for two-prong events. The shaded area indicates the selected quasielastic events. The dashed line represents the background. The curve is the prediction for the quasielastic events from Monte Carlo simulation.

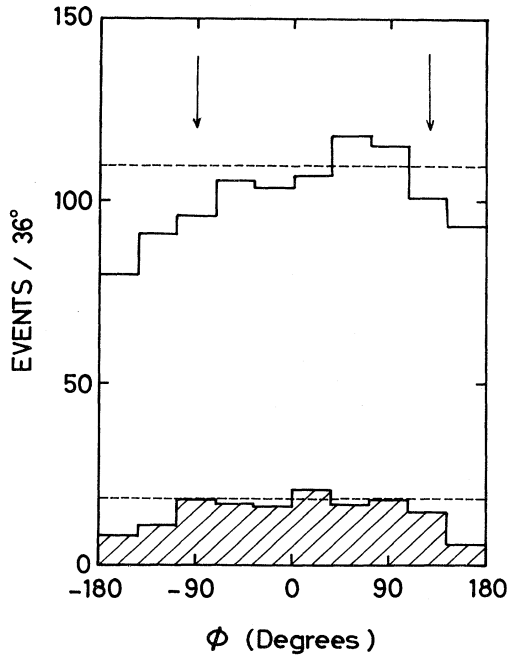

FIG. 4. The distribution of the azimuthal angle ϕ for the proton p in $\nu_\mu d \to \mu^- p p_s$ events with $Q^2 > 0.1$ GeV^2; here ϕ is the azimuthal angle in a plane perpendicular to $\vec{P}_\nu$ measured from the plane containing a camera and $\vec{P}_\nu$. The shaded area corresponds to the additional events found in the rescan.

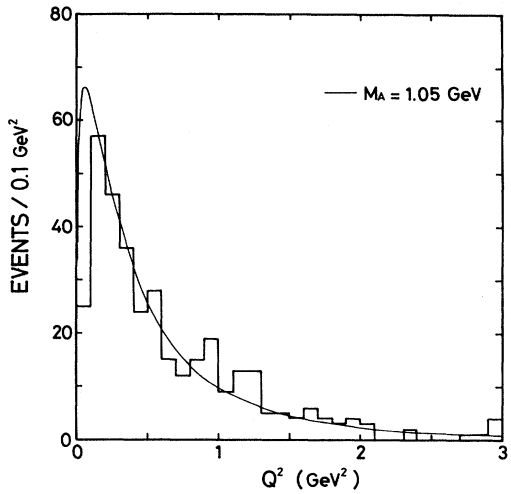

FIG. 5. The Q^2 distribution for the selected quasielastic events. The solid curve represents the differential cross section of quasielastic scattering for the neutron in deuteron.

near $\phi=0°$. The shaded area corresponds to the additional events found from the rescan. Using the average of the events with ϕ between $-90°$ and $126°$ (dashed line), we calculated the event bias to be 8%. This does not necessarily represent the true loss of events because of the three-point plot per event. We examined the true event loss from the event bias in Fig. 4 by using a Monte Carlo simulation. This event loss amounts to 8% and is not recovered by rescanning (shaded area). Hence, a correction of 1.08 ± 0.05 has been made to the data independent of scanning efficiency.

Figure 5 shows the Q^2 distribution for the quasielastic events. The curve in Fig. 5 is the best fit obtained by using the prediction of the differential cross section for reaction (2) with $M_A=1.05$ GeV which was obtained from this experiment (see Sec. III). The χ^2 value from this fit was found to be 15 for 20 data points for Q^2 between 0.1 and 3 GeV^2. Comparing the observed Q^2 distribution to the fitted curve, the correction factor for $Q^2<0.1$ GeV^2 is estimated to be 1.10 ± 0.02. The overall correction factor including scanning-measuring efficiency is 1.34 ± 0.07. We note that this correction factor influences the value of the neutrino flux but not the M_A value, because we use a flux-independent method[2] to determine M_A.

III. MEASUREMENT OF THE FORM FACTOR

In the context of the $V-A$ theory, the matrix element for the quasielastic reaction, $\nu_\mu n \to \mu^- p$, can be written as a product of the hadronic weak current and the leptonic current.[14] The general form of the hadronic weak current is written in terms of six complex form factors which are functions of Q^2 and characterize the nucleon structure. These are F_S (induced scalar), F_p (induced pseudoscalar), F_V^1 (isovector Dirac), F_V^2 (isovector Pauli), F_A (axial vector), and F_T (induced tensor). The quasielastic cross section can be expressed in terms of these six form factors.

In order to simplify the analysis of the quasielastic reaction, the following assumptions are made: (1) time-reversal invariance and charge symmetry, (2) partially conserved axial-vector current (PCAC) for the small pseudoscalar term, and (3) isotriplet-conserved-vector-current (CVC) hypothesis.

The first assumption, which requires all form factors to be real, yields $F_S=F_T=0$, leading to the absence of second class currents. With the second assumption, $F_P(Q^2)$ is given by

$$F_P(Q^2)=2M^2F_A(Q^2)/(Q^2+m_\pi^2)\ , \tag{4}$$

where

$$Q^2=(\vec{\mathrm{P}}_\nu-\vec{\mathrm{P}}_\mu)^2-(E_\nu-E_\mu)^2\ .$$

The contribution to the cross section from this term in the energy region $E_\nu>5$ GeV is less than 0.1%, and consequently this term is neglected. The third assumption relates F_V^1 and F_V^2 to the isovector Sachs electric and magnetic form factor, G_E and G_M determined from electron-scattering experiments as follows:

$$F_V^1(Q^2)=\left[G_E(Q^2)+\frac{Q^2}{4M^2}G_M(Q^2)\right]\left[1+\frac{Q^2}{4M^2}\right]^{-1},$$

$$F_V^2(Q^2)=[G_M(Q^2)-G_E(Q^2)]\xi^{-1}\left[1+\frac{Q^2}{4M^2}\right]^{-1}, \tag{5}$$

$$G_E(Q^2)=G_M(Q^2)(1+\xi)^{-1}=\lambda(Q^2)\left[1+\frac{Q^2}{M_V^2}\right]^{-2},$$

where M_V is the vector mass, $M_V=0.84$ GeV, ξ is the difference between the proton and neutron anomalous magnetic moment,

$$\xi=\mu_p-\mu_n=3.708\ ,$$

and $\lambda(Q^2)$ (Ref. 15) is the correction factor for the small deviation of the electron-scattering data from a pure dipole form factor. We further assume the axial-vector form factor in a dipole form,

$$F_A(Q^2)=F_A(0)/(1+Q^2/M_A^2)^2\ , \tag{6}$$

where the value of $F_A(0)=-1.23\pm0.01$ is taken from β-decay experiments.[16]

From these assumptions, the differential cross section for the quasielastic reaction can be expressed in terms of only one parameter, M_A, as

$$\frac{d\sigma}{dQ^2}=\frac{G^2M^2\cos^2\theta_C}{8\pi E_\nu^2}\left[A(Q^2)+B(Q^2)\frac{(s-u)}{M^2}+C(Q^2)\frac{(s-u)^2}{M^4}\right], \tag{7}$$

where $s-u=4ME_\nu-Q^2-m_\mu^2$, and $M=(M_n+M_p)/2$. The values of the Fermi constant and of the Cabibbo angle are taken to be $G=1.166\,32\times10^{-5}$ GeV^{-2} and $\cos\theta_C=0.9737$, respectively (see Ref. 16). The structure

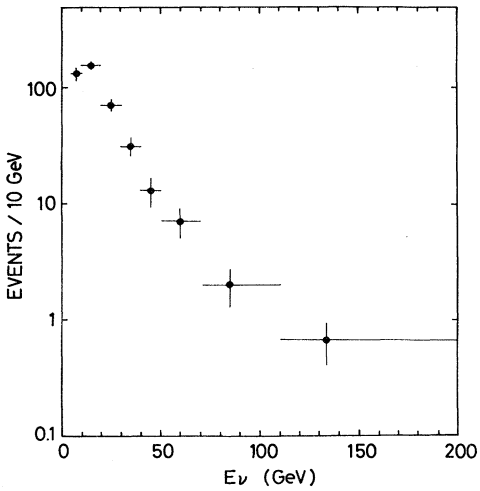

FIG. 6. The E_ν distribution for the selected quasielastic events.

functions A, B, and C are given in terms of F_V^1, F_V^2, and F_A:

$$A=\frac{Q^2}{4M^2}\left[\left(4+\frac{Q^2}{M^2}\right)|F_A|^2-\left(4-\frac{Q^2}{M^2}\right)|F_V^1|^2+\frac{Q^2}{M^2}\left(1-\frac{Q^2}{4M^2}\right)|\xi F_V^2|^2+\frac{4Q^2}{M^2}(F_V^1\xi F_V^2)\right],$$

$$B=-\frac{Q^2}{M^2}F_A(F_V^1+\xi F_V^2), \tag{8}$$

and

$$C=\frac{1}{4}\left(|F_A|^2+|F_V^1|^2+\frac{Q^2}{4M^2}|\xi F_V^2|^2\right).$$

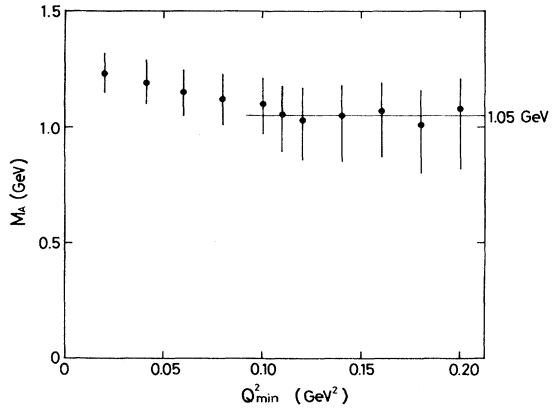

FIG. 7. $Q^2{}_{\min}$ effect on M_A.

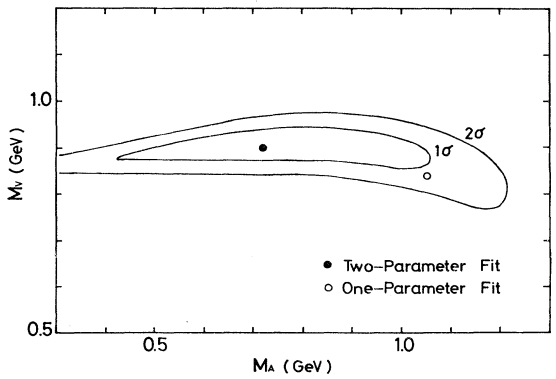

FIG. 8. Contour for one and two standard deviations in (M_A,M_V) space.

In this expression, terms proportional to $(m_\mu/M)^2$ are ignored.

The Q^2 and the neutrino energy distributions for the 362 quasielastic events are displayed in Figs. 5 and 6. The E_ν distribution decreases sharply with E_ν, extending to 200 GeV. In the Q^2 distribution, a depletion of events is seen at small Q^2 values. This is to be expected since such events have a low-momentum recoil proton and will appear as one-prong events. To obtain M_A from the Q^2 distribution for each observed neutrino energy E_ν^i, we used the flux-independent method,[2] defining a likelihood function

$$L=\prod_{i=1}^{N}\frac{d\sigma}{dQ^2}(Q_i{}^2,E_\nu^i,M_A)R(Q_i{}^2)/\Sigma\,. \tag{9}$$

Here N is the total number of quasielastic events in the Q^2 range between $Q^2{}_{\min}$ and $Q^2{}_{\max}$. $R(Q^2)$ is the correction factor for the cross section due to the effects of the Pauli

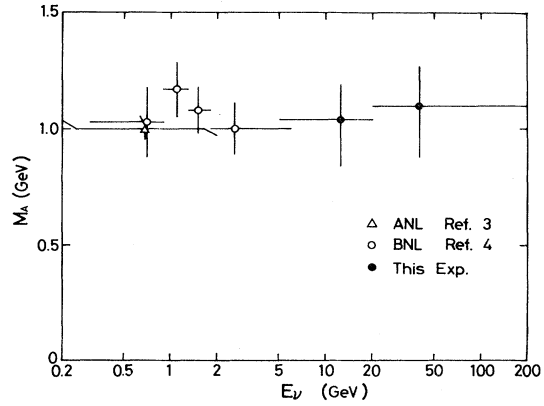

FIG. 9. The axial-vector mass M_A as a function of neutrino energy. The open circles (triangles) represent data of Ref. 2 (Ref. 4). Data of this experiment are displayed as the full circles.

TABLE I. Values of M_A as a function of neutrino energy.

E_ν (GeV)	$\langle E_\nu \rangle$ (GeV)	Events	M_A (GeV)	Reference
5—20	12.6	220	$1.04^{+0.15}_{-0.20}$	
20—200	40.0	142	$1.10^{+0.17}_{-0.22}$	This experiment
5—200	26.9	362	$1.05^{+0.12}_{-0.16}$	
0.15—3	~0.7	1737	1.00±0.05	3
0.3—0.9	0.69	256	1.03±0.15	4
0.9—1.3	1.08	302	1.17±0.12	4
1.3—1.8	1.52	295	1.08±0.10	4
1.8—6.0	2.55	285	1.00±0.11	4

exclusion principle and the Fermi motion in the deuteron.[17] The normalization factor is expressed as

$$\Sigma = \int_{Q^2_{\min}}^{Q^2_{\max}} \frac{d\sigma}{dQ^2}(Q^2, E_\nu^i, M_A) R(Q^2) dQ^2 . \quad (10)$$

Varying the $Q^2{}_{\min}$ cut values, we performed maximum likelihood fits to the data with a fixed value of $M_V = 0.84$ GeV.[14] The results of these fits are displayed in Fig. 7, where the effect on M_A due to the event depletion in the small-Q^2 region is observed. For $Q^2{}_{\min} > 0.11$ GeV^2, the fitted M_A value remains constant, indicating no effect from the low-Q^2 event loss. Thus, we determine the M_A value at $Q^2{}_{\min} = 0.1$ GeV^2 to be

$$M_A = 1.05^{+0.12}_{-0.16} \text{ GeV} ,$$

where the errors correspond to a change in L from the maximum value $L^{\max}$ to $0.5L^{\max}$. This mass value is consistent with values measured in earlier low energy experiments.[1–4]

A least squares fit to the Q^2 distribution was also performed for Q^2 between 0.1 and 3.0 GeV^2. The result of the best fit gives $M_A = 1.01$ GeV which is consistent with the value obtained from the maximum likelihood method. We also performed a two-parameter fit using dipole forms for both $F_A(Q^2)$ and $F_V(Q^2)$, in which M_A and also M_V were allowed to vary. Figure 8 shows the contour plots of the likelihood values in the (M_A, M_V) space. This fit yields $M_A = 0.72^{+0.34}_{-0.20}$ GeV and $M_V = 0.90 \pm 0.05$ GeV, which are consistent with the value of M_A obtained from the one-parameter fit.

In the high-energy limit, Eq. (7) approaches

$$\frac{d\sigma}{dQ^2} = \frac{G^2 \cos^2\theta_C}{2\pi} \left[|F_A|^2 + |F_V^1|^2 + \frac{Q^2}{M^2} |\xi F_V^2|^2 \right] . \quad (11)$$

Hence, any energy dependence of the form factors in Eq. (11) would be directly reflected in the value of M_A through $|F_A|^2$ if the theoretical formulation were not appropriate. Figure 9 and Table I show the results of the one-parameter fits for two energy regions in our experiment, together with the data from the low-energy experiments.[3,4] These results indicate no energy dependence of F_A, F_V^1, and F_V^2, supporting the $V-A$ formulation at higher energies.

In Table II, we summarize the values of M_A obtained from the recent $\nu_\mu d$ experiments[3,4] together with the value from this experiment. The weighted average value of M_A is now

$$M_A = 1.03 \pm 0.04 \text{ GeV} ,$$

which is somewhat lower than the value of $M_A \sim 1.15$ GeV obtained from the electroproduction experiments.[5]

Figure 10 shows the quasielastic cross section as a function of E_ν. The data points from this experiment and the Brookhaven data points[4,18] were calculated from Eq. (7) using the M_A values in Table I, while the low-energy data[2] were obtained by using the absolute neutrino flux measurement. The curve is the prediction calculated from Eq. (7) with $M_A = 1.05$ GeV. We note that the high-energy data connect smoothly with the low-energy data.

VI. SUMMARY

We have studied the quasielastic neutrino reaction $\nu_\mu n \to \mu^- p$ in a high-energy neutrino exposure of the Fer-

TABLE II. M_A values obtained from the $\nu_\mu d$ experiments.

E_ν (GeV)	Events	M_A (GeV)	
0.15— 3	1737	1.00 ±0.05	Ref. 3
0.3 — 6	1138	1.070±0.057	Ref. 4
5 —200	362	$1.05^{+0.12}_{-0.16}$	This experiment
0.15—200	3237	1.032±0.036	Average

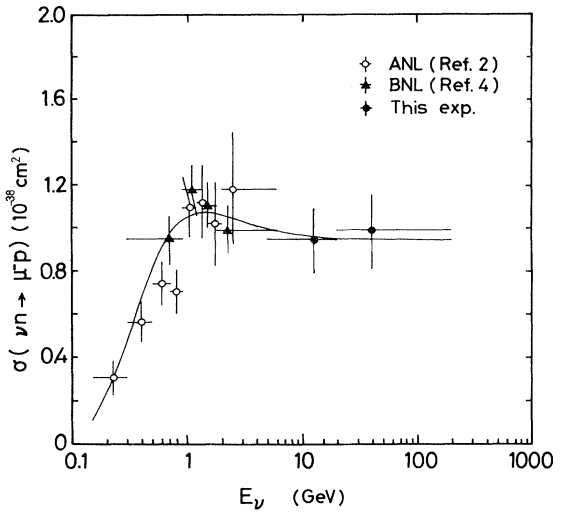

FIG. 10. Quasielastic cross section $\sigma(\nu_\mu n \to \mu^- p)$ as a function of E_ν. The data points from this experiment and Ref. 4 are calculated from Eq. (7) using the M_A values in Table I. The curve is derived from Eq. (7) with $M_A = 1.05$ GeV.

milab 15-ft deuterium-filled bubble chamber to a wide-band neutrino beam. A total of 362 quasielastic events were found in the 16.7-m^3 fiducial volume, from the analysis of 96% of the total exposure. In the dipole parametrization of the axial-vector form factor of the nucleon, we measured the axial-vector mass to be $M_A = 1.05^{+0.12}_{-0.16}$ GeV, which is consistent with the previous low-energy measurements. A search for an energy dependence of M_A showed no clear energy dependence, supporting the assumptions and the $V-A$ formulation used for the quasielastic reaction in our energy range (5—200 GeV).

ACKNOWLEDGMENTS

We thank the members of the Accelerator Division and Neutrino Department at Fermilab for their assistance. We also wish to thank our scanning and measuring personnel for their dedicated effort. This research is supported in part by the U. S. Department of Energy and the National Science Foundation.

*Present address: Columbia University, New York, New York 10027.

†On leave from the University of Warsaw, 00-681 Warsaw, Poland.

‡Present address: Bell Telephone Laboratories, Naperville, Illinois 60540.

§Present address: University of Notre Dame, Notre Dame, Indiana 46556.

[1]M. M. Block *et al.*, Phys. Lett. 12, 281 (1964); A. Orkin-Lecourtois and C. A. Piketty, Nuovo Cimento 50A, 927 (1967); M. Holder *et al.*, *ibid.* 47A, 338 (1968); R. L. Kustom *et al.*, Phys. Rev. Lett. 22, 1014 (1969); I. Budagov *et al.*, Lett. Nuovo Cimento 2, 689 (1969); S. Bonetti *et al.*, Nuovo Cimento 38A, 260 (1977). See also M. DeWit, in *Proceedings of Topical Conference on Neutrino Physics at Accelerators, Oxford, 1978*, edited by A. G. Michelle and P. B. Renton (Rutherford Laboratory, Chilton, Didcot, Oxfordshire, England, 1978), p. 75.

[2]W. A. Mann *et al.*, Phys. Rev. Lett. 31, 844 (1973); S. J. Barish *et al.*, Phys. Rev. D 16, 3103 (1977).

[3]K. L. Miller *et al.*, Phys. Rev. D 26, 537 (1982).

[4]N. J. Baker *et al.*, Phys. Rev. D 23, 2499 (1981).

[5]E. Amaldi *et al.*, Phys. Lett. 41B, 216 (1972); E. D. Bloom *et al.*, Phys. Rev. Lett. 30, 1186 (1973); P. Branel *et al.*, Phys. Lett. 45B, 386 (1973); A. del Geurra *et al.*, Nucl. Phys. B107, 65 (1976); P. Joos *et al.*, Phys. Lett. 62B, 230 (1976).

[6]T. Kitagaki *et al.*, Phys. Rev. Lett. 45, 955 (1980); T. Kitagaki *et al.*, *ibid.* 48, 299 (1982).

[7]J. Hanlon *et al.*, Phys. Rev. Lett. 45, 1817 (1980).

[8]T. Kitagaki *et al.*, Phys. Lett. 97B, 325 (1980).

[9]T. Kafka *et al.*, Phys. Rev. Lett. 48, 910 (1982).

[10]T. Kitagaki *et al.*, Phys. Rev. Lett. 49, 98 (1982); D. Son *et al.*, *ibid.* 49, 1128 (1982), D. Zieminska *et al.*, Phys. Rev. D 27, 47 (1983).

[11]S. Mori, Fermilab Report No. TM-720, 1977 (unpublished); J. Grimson and S. Mori, Fermilab Report No. TM-824, 1978 (unpublished).

[12]Lamek Hulthen and Masao Sugawara, *Handbuch der Physik* (Springer, Berlin, 1957), Vol. 39, Chap. 1; J. S. Danburg *et al.*, Phys. Rev. D 2, 2564 (1970).

[13]For details of the method used see T. Kafka *et al.*, Phys. Rev. D 19, 76 (1979).

[14]C. H. Llewellyn Smith, Phys. Rep. 3C, 261 (1972); R. E. Marshak, Riazuddin, and C. P. Ryan, *Theory of Weak Interactions in Particle Physics* (Wiley-Interscience, New York, 1969). Also see references therein.

[15]M. G. Olsson, E. T. Osyporeski and E. H. Monsay, Phys. Rev. D 17, 2938 (1978).

[16]Particle Data Group, Rev. Mod. Phys. 52, S1 (1980).

[17]S. K. Singh, Nucl. Phys. B36, 419 (1971).

[18]N. P. Samios and M. Tanaka (private communication).